

# Advanced electron microscopic techniques provide a deeper insight into the peculiar features of podocytes

Tillmann Burghardt,<sup>1</sup> Florian Hochapfel,<sup>1</sup> Benjamin Salecker,<sup>1</sup> Christine Meese,<sup>1</sup> Hermann-Josef Gröne,<sup>2</sup> Reinhard Rachel,<sup>3</sup> Gerhard Wanner,<sup>4</sup> Michael P. Krahn,<sup>1</sup> and Ralph Witzgall<sup>1</sup>

<sup>1</sup>Institute for Molecular and Cellular Anatomy, University of Regensburg, Regensburg, Germany; <sup>2</sup>Division of Cellular and Molecular Pathology, German Cancer Research Center, Heidelberg, Germany; <sup>3</sup>Center of Electron Microscopy, Faculty of Biology and Preclinical Medicine, University of Regensburg, Regensburg, Germany; and <sup>4</sup>Department of Botany, Ludwig Maximilians-Universität, Munich, Germany

Submitted 28 July 2015; accepted in final form 17 September 2015

**Burghardt T, Hochapfel F, Salecker B, Meese C, Gröne H, Rachel R, Wanner G, Krahn MP, Witzgall R.** Advanced electron microscopic techniques provide a deeper insight into the peculiar features of podocytes. *Am J Physiol Renal Physiol* 309: F1082–F1089, 2015. First published September 23, 2015; doi:10.1152/ajprenal.00338.2015.—Podocytes constitute the outer layer of the glomerular filtration barrier, where they form an intricate network of interdigitating foot processes which are connected by slit diaphragms. A hitherto unanswered puzzle concerns the question of whether slit diaphragms are established between foot processes of the same podocyte or between foot processes of different podocytes. By employing focused ion beam-scanning electron microscopy (FIB-SEM), we provide unequivocal evidence that slit diaphragms are formed between foot processes of different podocytes. We extended our investigations of the filtration slit by using dual-axis electron tomography of human and mouse podocytes as well as of *Drosophila melanogaster* nephrocytes. Using this technique, we not only find a single slit diaphragm which spans the filtration slit around the whole periphery of the foot processes but additional punctate filamentous contacts between adjacent foot processes. Future work will be necessary to determine the proteins constituting the two types of cell-cell contacts.

podocyte

PODCYTES REPRESENT THE OUTERMOST cell layer of the glomerular filtration barrier. Based on results obtained with conventional imaging techniques, the current model pictures the podocyte cell body as floating in Bowman's space while being anchored to the glomerular basement membrane via its arborizing cellular extensions. The finest branches, the foot processes, are arranged in an interdigitating pattern on the outer surface of the basement membrane (11). Neighboring foot processes are connected by a slit diaphragm which supposedly contains the integral membrane proteins nephrin, Neph1, FAT-1, and P-cadherin. These proteins are linked to the actin cytoskeleton through the adapter proteins podocin, CD2AP, and zonula occludens (ZO)-1 (17). It has been suggested that the urinary space between the podocyte and the glomerular basement membrane, the subpodocyte space, impedes the flow of the primary filtrate into Bowman's space and that therefore the subpodocyte space contributes to the filtration properties of the renal glomerulus (8, 9, 13). Hereditary and acquired podocytopathies lead to the destruction of the intricate cytoarchitecture of podocytes and consequently to a failure of the renal filter. The

hallmark of such podocytopathies is the disappearance of foot processes and ultimately a detachment of affected podocytes into the urine, thus causing albuminuria (7, 15).

The current view on the structural basis of the renal filtration barrier was derived from classic transmission and scanning electron microscopy. While these techniques have provided valuable information, they also suffer from intrinsic limitations and therefore leave open fundamental questions: 1) What is the dimension of a single podocyte? 2) How are podocytes arranged on the glomerular basement membrane? and 3) Does a podocyte form slit diaphragms between its own foot processes? To answer these questions, we applied novel electron microscopic techniques, i.e., focused ion beam-scanning electron microscopy and dual-axis electron tomography, to podocytes from several species. This made it possible to obtain detailed information on the spatial arrangement of an entire podocyte in its intact environment including visualization of the subpodocyte space.

## MATERIALS AND METHODS

**Scanning electron microscopy.** Preparation of the kidneys for scanning electron microscopy was done according to Tanaka et al. (16) with modifications. Mice were perfusion-fixed with 4% paraformaldehyde/1× PBS through the distal abdominal aorta for 3 min. Kidneys were cut in half and incubated for 2 h in 2% glutaraldehyde/0.1 M Na cacodylate, pH 7.4, followed by overnight impregnation in 30% dimethylformamide at 4°C. Freeze fracturing was performed with a cold knife under liquid nitrogen followed by immersion in dimethylformamide at room temperature for 2 h. Finally, image data were acquired on a Zeiss LEO 1530 Gemini scanning electron microscope using the SE2 detector (Carl Zeiss Microscopy, Oberkochen, Germany).

**Focused ion beam-scanning electron microscopy.** Perfusion-fixation of adult mice was done as described for scanning electron microscopy. Kidneys were stored at 4°C in 2% glutaraldehyde/0.1 M Na cacodylate, pH 7.4, overnight. Then, the tissues were incubated with 0.1 M cacodylate-buffered 1% OsO<sub>4</sub> for 4 h, followed by dehydration in an ethanol series at room temperature and Epon embedding.

Acquisition of tomographic data sets was performed on a Zeiss Auriga 60 dual-beam workstation (Carl Zeiss Microscopy). Slicing of the Epon block was set to a step size of 15 nm and a focused ion beam milling current of 1 nA with a Ga-emitter voltage at 30 kV. Scanning electron microscopic data were recorded in the high-current mode at 1.5 kV of the in-lens EsB detector with an aperture of 60 μm. The dimensions of the recorded images were 2,048 × 1,536 pixels, with a pixel size of 15 nm. The slice and view process was repeated 1,652 times to obtain the 3-dimensional dataset. Raw data were binned and aligned using the open source software package ImageJ (14). Seg-

Address for reprint requests and other correspondence: R. Witzgall, Univ. of Regensburg, Institute for Molecular and Cellular Anatomy, Universitätsstr. 31, 93053 Regensburg, Germany (e-mail: ralph.witzgall@vkl.uni-regensburg.de).

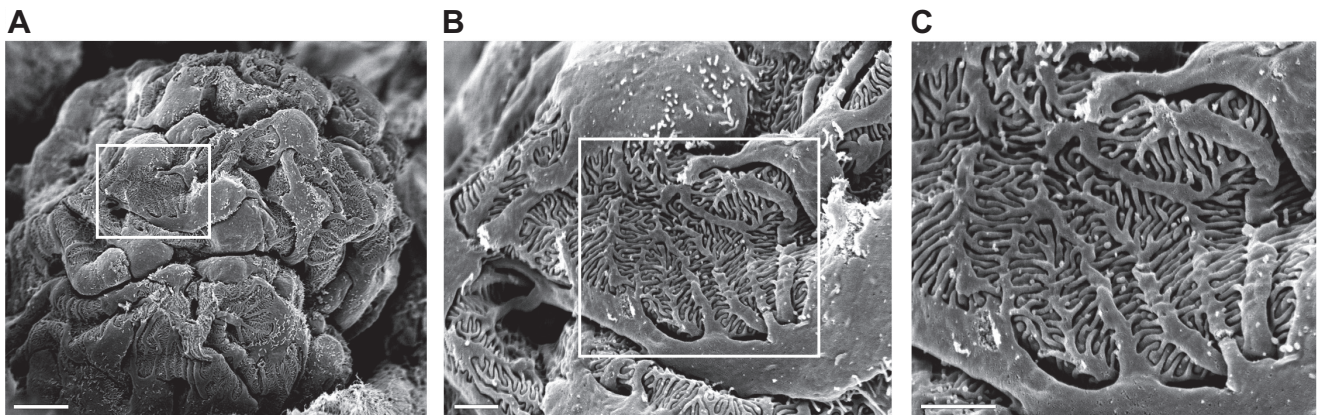


Fig. 1. Scanning electron micrograph of a normal glomerulus. The micrograph was taken from the glomerulus of a 3-mo-old C57BL/6 mouse. It shows the intricate pattern of podocyte processes and illustrates that it is impossible by this technique to determine whether foot processes of the same podocyte do or do not interact with each other. Bars = 10  $\mu\text{m}$  (A) and 2  $\mu\text{m}$  (B and C).

mentation was performed manually using AMIRA (Visage Imaging, Berlin, Germany). The segmentation was smoothed by applying the “smooth labels” feature in the Label Field. One kidney was chosen for further analysis.

**Tissue preparation.** Perfusion fixation of murine kidneys was performed as described above. Mouse kidney biopsies were high pressure frozen (EM-PACT2, Leica, Wetzlar, Germany) and freeze-substituted in acetone/2%  $\text{OsO}_4$ /5%  $\text{H}_2\text{O}$ /0.25% uranyl acetate (AFS2, Leica). Finally, samples were embedded in Epon. Fine needle biopsies of human kidneys were fixed with 4% buffered formaldehyde and embedded in Araldite R. Stocks of *Drosophila melanogaster* were cultured on standard cornmeal agar and maintained at 25°C. Garland nephrocytes from wandering third instar larvae were microdissected in HL3.1 saline, high-pressure frozen, freeze-substituted, and embedded in Epon. Treatment of mice was conducted in accordance with the German Animal Protection Law and was approved by the local government. The use of human kidney biopsies was approved by the ethics committee of the University of Heidelberg.

**Electron tomography.** For the tilt series, 200- to 300-nm thick sections were cut using a diamond knife (Diatome, Biel, Switzerland) with an ultramicrotome (UC6 or UC7, Leica). The thickness of the sections was determined on the reconstructed three-dimensional volume (see below). The tilt series was recorded on a JEM-2100F transmission electron microscope (JEOL, Tokyo, Japan) operating at 200 kV with a nominal magnification of 20,000. Digital images were collected by a TVIPS F416 CMOS camera with an effective pixel size of 0.54 nm. The tilt series was recorded from  $-65^\circ$  to  $+65^\circ$  with an angular increment of  $1^\circ$ . The three-dimensional reconstructions were calculated using IMOD (6). Images were preprocessed, binned, and aligned using randomly distributed 10-nm gold particles as fiducial markers. The generation of tomograms was performed by the simultaneous iterative reconstruction technique (SIRT).

## RESULTS

**Foot processes of the same podocyte do not interdigitate with each other.** A regular scanning electron micrograph of a murine glomerulus shows the fine interdigitating foot processes of podocytes (Fig. 1). From these pictures, however, it is impossible to determine whether foot processes of the same podocyte interact with each other. To answer this long-standing question, we decided to reconstruct a complete murine podocyte based on focused ion beam-scanning electron microscopy (FIB-SEM). In FIB-SEM, a gallium beam mills off 10- to 20-nm-thick layers of a plastic-embedded tissue sample, which is followed by scanning electron microscopy of the surface

after each round of milling. This way, large z-stacks of the desired objects can be created. In our analysis of a murine podocyte, we have created a  $29.6 \times 22.3 \times 24.0\text{-}\mu\text{m}$  three-dimensional stack at 15-nm intervals. In portraying our results, we define primary processes as branches originating directly from the podocyte cell body without interdigitating with other processes, secondary processes as branches originating from primary processes without interdigitating with other processes, tertiary processes as branches originating from secondary processes without interdigitating with other processes, and foot processes as protrusions interdigitating with other foot processes (Fig. 2). Foot processes may originate from all kinds of other processes and even from the cell body (Fig. 2). The podocyte at the center of our 3-dimensional analysis elaborates 12 primary processes and 44 secondary processes; it spreads out over several capillaries (Figs. 2 and 3).

The space between podocytes and the underlying glomerular basement membrane, i.e., the subpodocyte space, has gained recent attention because it may represent an additional mechanism regulating the flow of the primary filtrate (9, 13). Our three-dimensional reconstruction shows an elaborate labyrinth below the podocyte cell body (Fig. 4A) with narrow exit sites

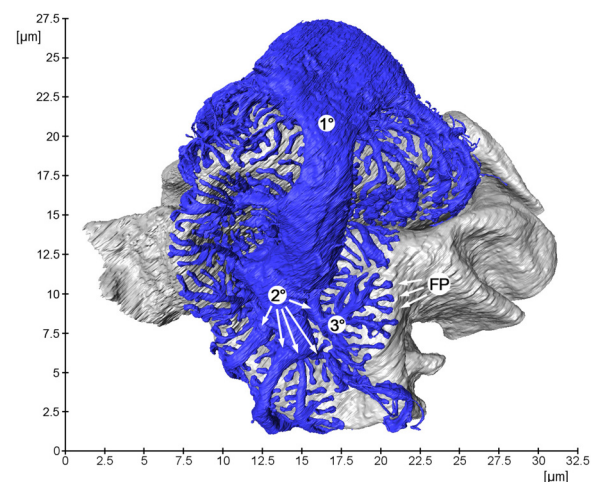


Fig. 2. Three-dimensional reconstruction of a murine podocyte. On this side of the reconstructed cell, the primary (1°), secondary (2°), tertiary (3°), and foot processes (FP) can be seen. The capillaries are shown in grey.

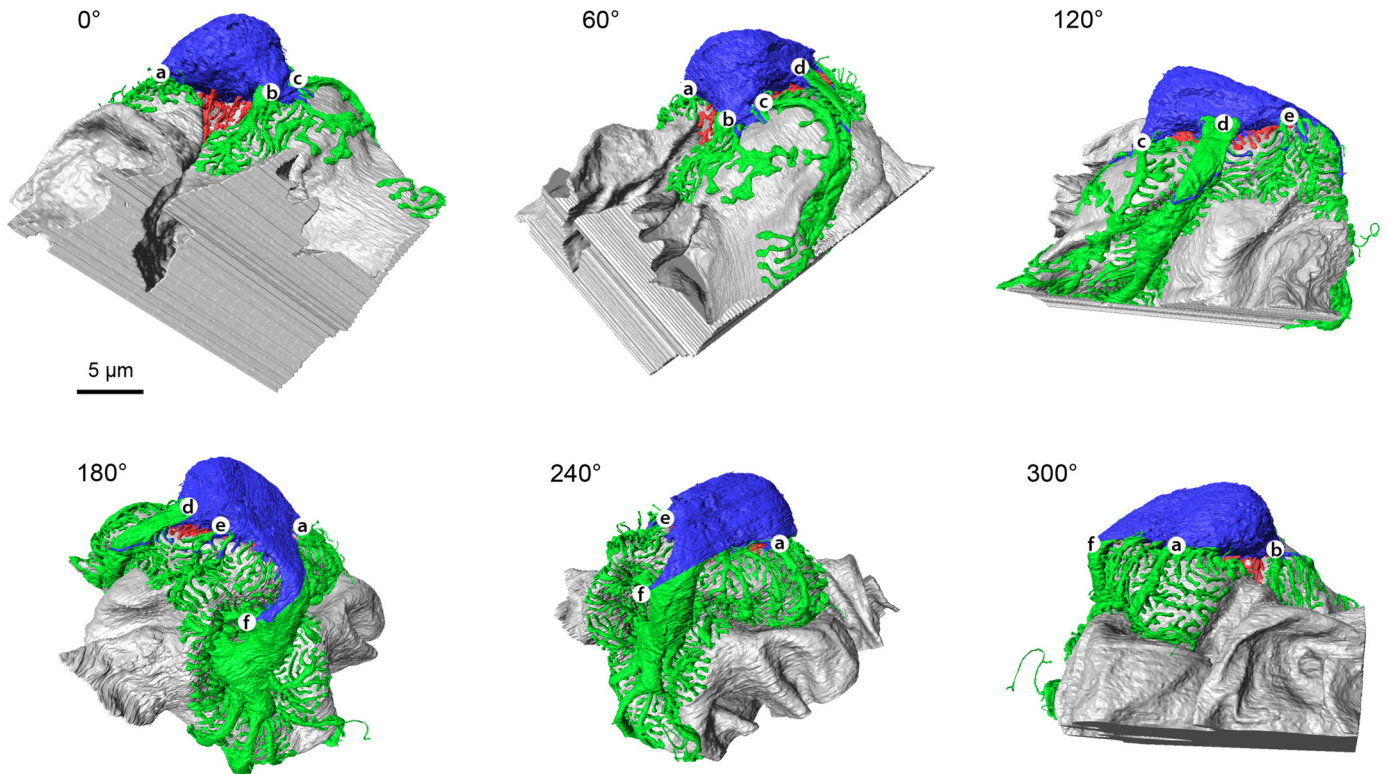


Fig. 3. Three-dimensional reconstruction of a murine podocyte. The same podocyte as in Fig. 2 is shown. It was rotated in 60° intervals to better demonstrate its extensive processes. The cell body is shown in blue, processes extending sideways in green, and processes extending from the basal surface of the cell body in red; the capillaries are shown in grey. The letters *a–f* were inserted for better orientation and do not reflect the processes.

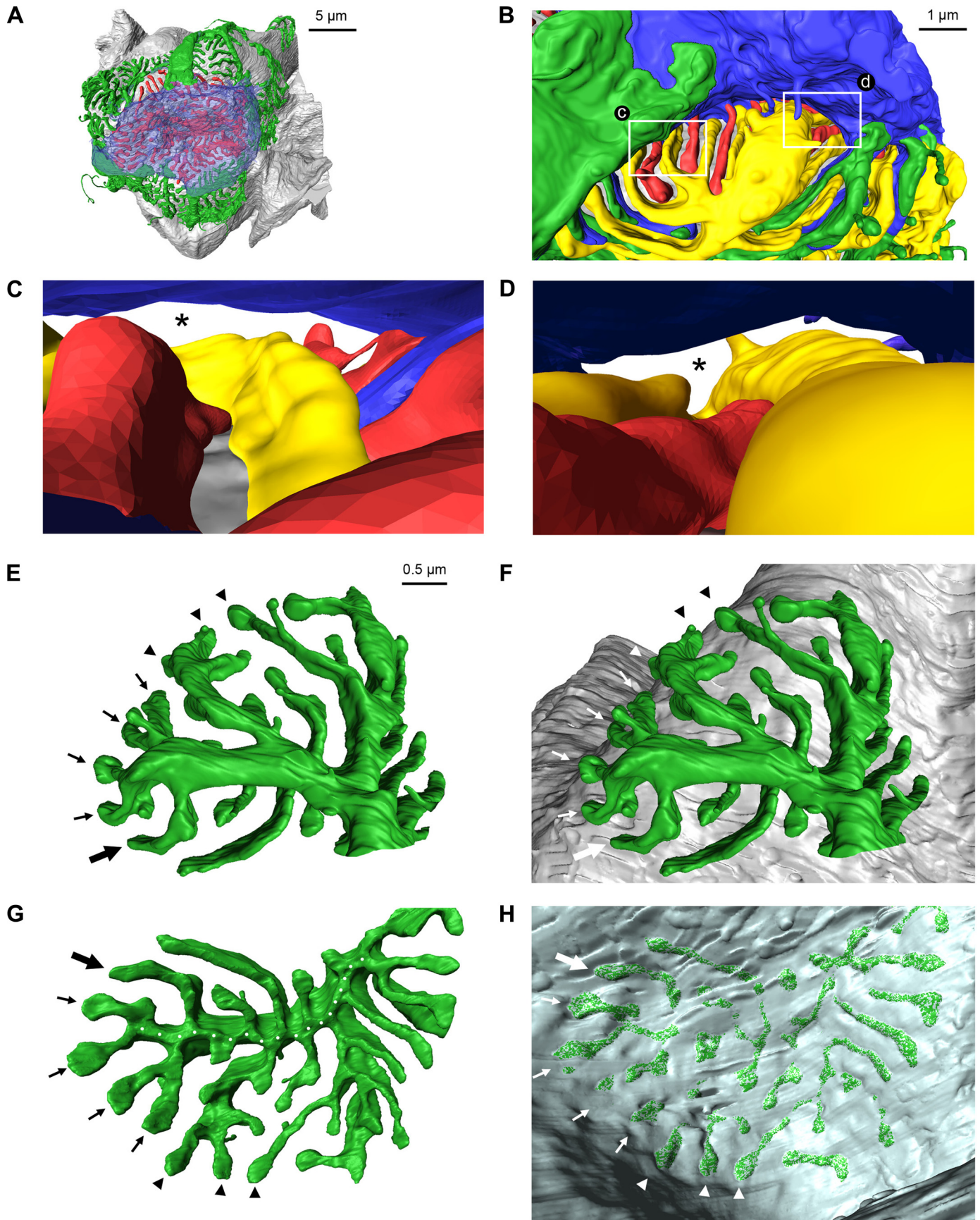
flanked by the cell body and the adjacent processes (Fig. 4, *B–D*). As has been suggested before by conventional transmission electron microscopy, the cell body of the podocyte does not sit broadly on the glomerular basement membrane. However, contrary to what has been called the freely floating cell body of the podocyte, we detected a number of processes extending directly from the basal surface, thus anchoring the podocyte cell body to the glomerular basement membrane (Fig. 4*A*). Furthermore, the major processes are also anchored to the basement membrane. When viewed from the glomerular basement membrane, we were able to see the ridge-like prominences which have recently been described in rat podocytes (4). These ridges lie in an intimate spatial relationship with the glomerular basement membrane and may help to anchor the major processes to the extracellular matrix (Fig. 4, *E–H*).

One crucial issue in podocyte biology concerns the question of whether slit diaphragms form between foot processes of the same podocyte or between foot processes of different podocytes. Our analysis clearly demonstrates that foot processes of the same podocyte do not interdigitate which each other and

therefore slit diaphragms only connect foot processes of different podocytes (Fig. 5).

*Electron tomographic characterization of connections between neighboring foot processes.* In previous publications, more than one cell-cell contact has been described between adjacent foot processes (5, 18); these contacts have been interpreted as multiple layers of the slit diaphragm. Indeed, we were able to recapitulate by conventional electron microscopy that multiple cell-cell contacts existed between foot processes of murine and human podocytes, and this was true as well for nephrocytes of the fly *D. melanogaster*. As a matter of fact, only in a minority of filtration slits a single cell-cell contact was seen (~20% of filtration slits in the mouse, ~10% of filtration slits in human and the fly) (Fig. 6*A*). Since some of the filtration slits were not represented in their entirety in our sections, it is likely that the frequency of filtration slits with only a single cell-cell contact is even lower. We would like to emphasize that the three specimens were generated by very different protocols. The mouse kidneys were perfusion-fixed, high-pressure frozen, and freeze-substituted. In the case of the

Fig. 4. Illustration of the subpodocyte space and of the ridge-like prominences. The same podocyte as in Fig. 2 is shown. Its cell body is shown in blue, processes extending sideways in green, and processes extending from the basal surface of the cell body in red; the capillaries are shown in grey. *A*: top view of the podocyte with the cell body made semitransparent demonstrates the many processes extending from the basal side of the cell body to the glomerular basement membrane. *B*: a second podocyte shown in yellow is added (view from Bowman’s space). White rectangles indicate the exit sites from the subpodocyte space, which are shown as *c* and *d*. *C* and *D*: view from the subpodocyte space into Bowman’s space demonstrates the narrow exit sites (asterisks) from the subpodocyte space into Bowman’s space. *E–H*: top view of one podocyte branch shown without (*E*) and with (*F*) the glomerular basement membrane illustrated in grey. A bottom view of the same branch demonstrates the ridge-like prominence (dotted line in *G*) which leaves an imprint in the glomerular basement membrane (*H*), thus demonstrating the close spatial relationship between the 2 structures. Arrowheads and small and large arrows have been inserted for better orientation.



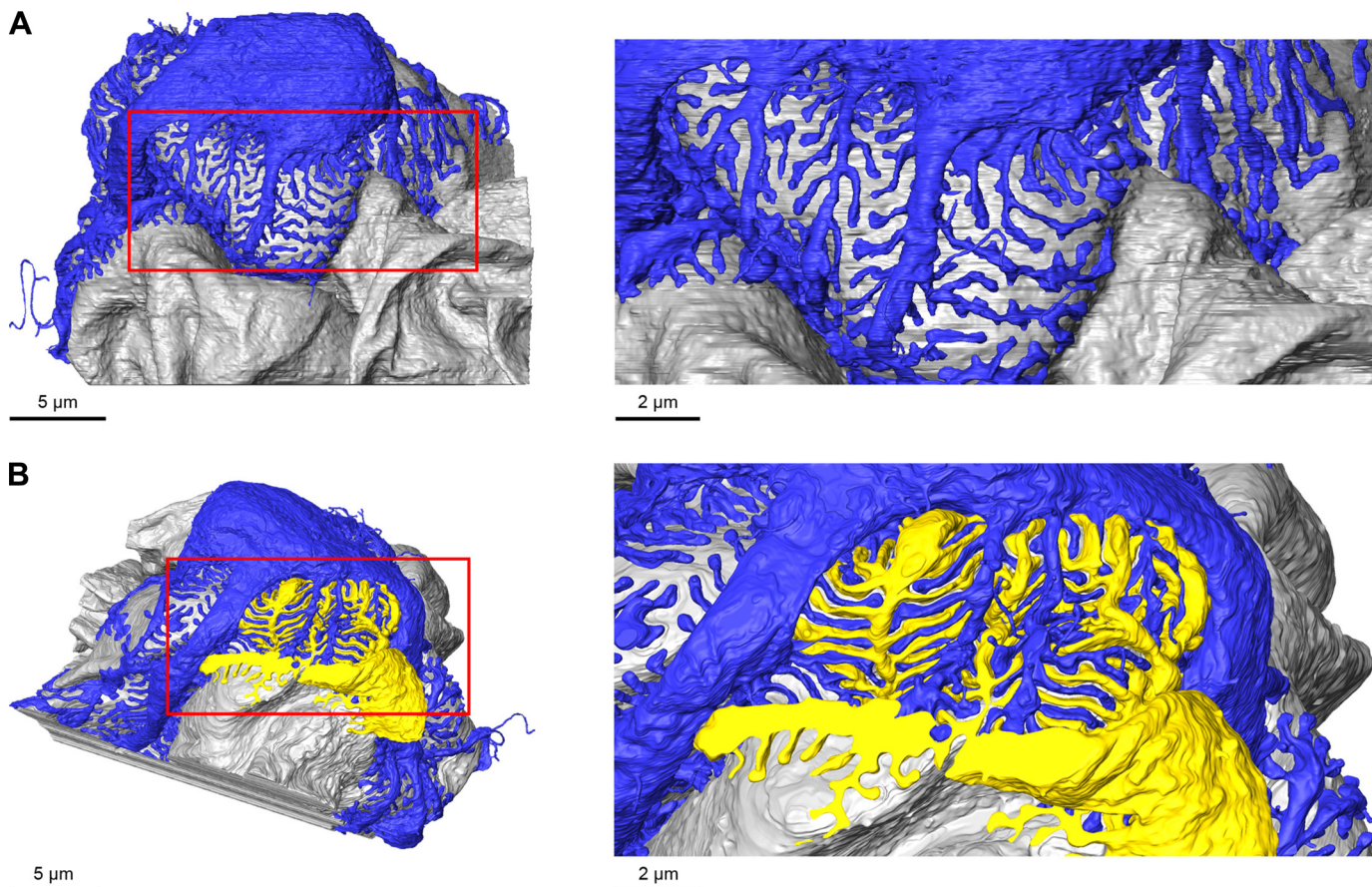


Fig. 5. Pattern of interdigitating foot processes. Shown in blue is the same podocyte as in Fig. 2 (for reasons of clarity both the cell body and the processes are shown in blue; the capillaries are shown in grey). In *A*, only the “blue” podocyte is illustrated, whereas in *B* a second “yellow” podocyte is inserted. The spaces between the blue foot processes are filled by the foot processes of the yellow podocyte, thus demonstrating the heterophilic interaction of podocyte foot processes. Red rectangles indicate the regions which are shown at more detail in the panels on the *right*.

human kidneys, needle biopsies were taken, and the biopsies were immersion-fixed and further processed at room temperature. Last, the fly nephrocytes were microdissected, high-pressure frozen, and freeze-substituted. Therefore, we consider it unlikely that the protocols for processing the tissues and cells, or that species differences account for the observed phenomenon. However, due to the fact that conventional electron microscopic pictures originate from ultrathin sections of only 40- to 80-nm thickness it is impossible to be sure of the three-dimensional nature of the underlying cell-cell contacts. We therefore took a closer look at podocytes and nephrocytes by dual-axis electron tomography. Employing this technique, we were surprised to find two different categories of cell-cell contacts between neighboring foot processes. One layer (we never observed more than one) of the conventional slit diaphragm surrounded the whole periphery of foot processes, which is consistent with conventional thinking (Fig. 6, *B–E*). In addition, we detected multiple punctate filamentous cell-cell contacts both below and above the slit diaphragm of podocytes (Fig. 6, *B–D*), and above the slit diaphragm of nephrocytes (Fig. 6*E*).

#### DISCUSSION

Our data provide novel insight into the peculiar ultrastructure of podocytes by extending the conventional two-dimen-

sional electron microscopic analysis into a third dimension. One long-standing puzzle in the podocyte field concerns the question of whether foot processes of the same podocyte can interact with each other. Very recent light microscopic investigations have suggested that this is not the case (2, 3), but it has to be kept in mind that neighboring foot processes are separated by a slit with a width of only 40 nm, well below the resolution of conventional light microscopes. While this manuscript was prepared for submission, an article was published in which FIB-SEM tomography was used for the partial reconstruction of rat podocytes (4). Regrettably, however, the authors did not pay special attention to the question and therefore did not present any unequivocal evidence whether slit diaphragms form between foot processes of the same podocyte or between foot processes of different podocytes. Our ultrastructural reconstruction of a complete podocyte from an adult mouse clearly demonstrates that foot processes of the same podocyte do not form slit diaphragms between each other. This is very surprising and obviously raises the question of why such an arrangement is necessary and how it is achieved. If the foot processes of an individual podocyte would interact with each other (homophilic interaction), then podocytes would only be able to gather information locally. Through the interaction of foot processes originating from different podocytes (heterophilic interaction), the podocyte layer in essence would

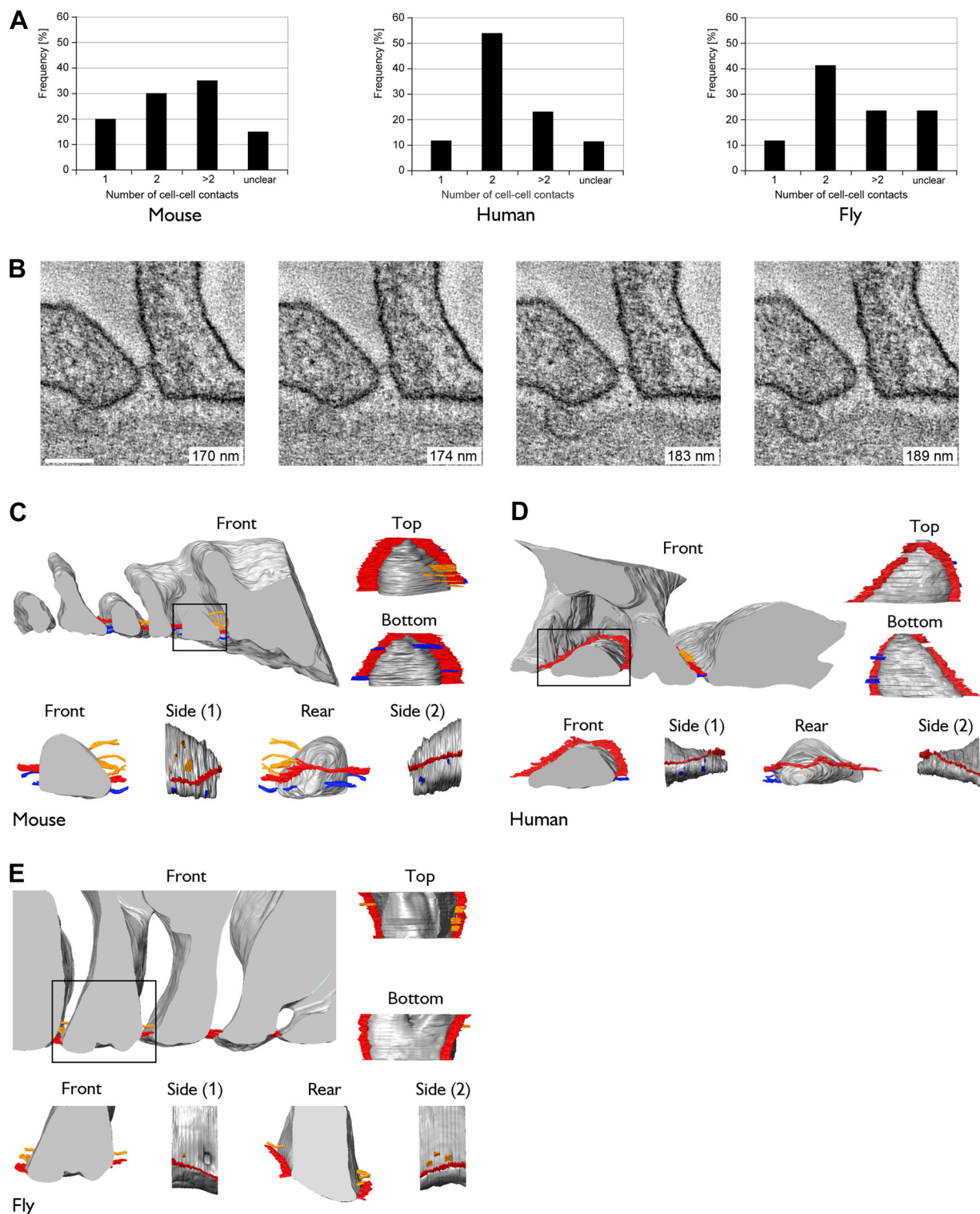


Fig. 6. Neighboring foot processes are connected by 2 types of cell-cell contacts. *A*: bar graph demonstrates the occurrence of filtration slits with single or multiple cell-cell contacts of murine and human podocytes and *Drosophila melanogaster* nephrocytes. *B*: example of a 2-layered cell-cell contact in a human specimen. The panels on the far left and far right show only a single contact, whereas the 2 panels in the middle show two cell-cell contacts. The numbers listed in the individual panels correspond to the level in the section, meaning that for example the first 2 pictures lie 4 nm apart. Bar = 100 nm. *C–E*: 3-dimensional view of the filtration slits from the 3 species. The slit diaphragms are shown in red, the filamentous cell-cell contacts above the slit diaphragm in yellow, and the filamentous cell-cell contacts below the slit diaphragm in blue. In *D*, it appears as if there is a break in the slit diaphragm when viewed from the top or the bottom. We cannot, however, rule out that this is a technical artifact.

form a network covering the capillaries whereby podocytes could collect information such as capillary pressure over large distances.

How can it be achieved that slit diaphragms form exclusively between foot processes of different podocytes? One possibility is that podocytes are not a homogeneous population of cells but that podocytes exist in distinct “flavors.” These populations would differ from each other by expressing different cell adhesion proteins which would not be able to establish homophilic interactions, i.e., foot processes of type “A” podocytes could not establish slit diaphragms between each other, and neither could foot processes of type “B” podocytes; instead, slit diaphragms would only form between type A and type B podocytes. Such a scenario is not completely unlikely because nephrin and Neph1, two integral membrane proteins of the slit diaphragm, preferentially interact in a heterophilic fashion (1). Regrettably, our attempts to stain kidney sections for nephrin and Neph1 to subject them to high-resolution stimulated emission depletion (STED) light microscopy failed, and we therefore were not able to determine whether nephrin and Neph1 are located in a mutually exclusive pattern on foot processes. Furthermore, it has been pointed out that a given podocyte not only interacts with one, but at least two other podocytes, which in such a model would require at least three different types of podocytes (see for example Fig. 1 in Ref. 4).

A more straightforward explanation comes from the pioneering work of Farquhar and colleagues (10). In their characterization of the morphological events underlying podocyte differentiation, they have described the transition of podocytes from simple columnar cells to extensively arborized cells. Already the columnar epithelial cells are connected to each other by tight junctions; due to their shape, these cells can only form tight junctions with neighboring cells and not with themselves. Upon differentiation, the prospective podocytes first elaborate rather coarse extensions which finally develop into the fine branches of the mature podocytes. During this process, cell-cell contacts apparently are maintained: the tight junctions move down from an apical to a basal location and are transformed into slit diaphragms. Since during this differentiation process a single podocyte never loses the cell-cell contacts with its neighbors, it follows automatically that slit diaphragms only form between neighboring cells. In principle, there is no reason why slit diaphragms cannot be established between foot processes of the same podocyte, and indeed this is true for *Drosophila*, where each nephrocyte is surrounded by its own basement membrane and nephrocytes do not interact with each other.

One other surprising result was the identification of two different types of cell-cell contacts between foot processes. Previous publications have described the occasional appearance of a supposedly two-layered slit diaphragm in human, rat, murine (18), and zebrafish glomeruli (5). In contrast, our data reveal the presence of only one layer of planar cell-cell contacts, i.e., the slit diaphragm, and of several additional punctate filamentous cell-cell contacts. Obviously, the misinterpretation in the previous publications was caused by looking only at conventional two-dimensional electron microscopic pictures. At present, we can only speculate on the nature and function of this novel type of contact. One rather trivial explanation would be that the filamentous cell-cell contacts represent transition states of the slit diaphragm, be it newly forming slit dia-

phragms or remnants of old slit diaphragms. Speaking against this hypothesis is the observation that despite the complete absence of slit diaphragms in patients suffering from mutations in the *NPHS1* gene, both regularly spaced filtration slits and altered filtrations slits were seen in the glomeruli of those patients (12). In a model in which the slit diaphragm is required to establish the regular spacing of foot processes, one has to wonder how normal appearing filtrations slits are generated when a slit diaphragm is not present at any time during kidney development. The authors of that publication (12) only mention “fuzzy cell surface material” between foot processes. It is quite feasible that the filamentous structures we describe in our current study have been missed in the patients’ kidney sections because conventional electron microscopy was performed and the kidney samples were not optimally preserved (kidney samples were obtained from aborted fetuses). We suggest that the filamentous cell-cell contacts we describe here are required to elaborate regularly spaced foot processes whereas the slit diaphragm would serve a sieving function and may possibly also be responsible for the formation of heterophilic cell-cell contacts.

The integral membrane proteins nephrin, Neph1, FAT-1, and P-cadherin are believed to be components of the slit diaphragm. These molecules belong to different families of cell-cell adhesion molecules: nephrin and Neph1 contain immunoglobulin-like domains, whereas FAT-1 and P-cadherin are members of the cadherin superfamily. Typically, only adhesion molecules of the same family are present in one type of cell-cell contacts, such as cadherins in adherens junctions. If all those different molecules contribute to the formation of slit diaphragms, they would have to interact in one form or another to maintain a tight slit diaphragm. So far, this has not been demonstrated. We also would like to point out that all of them have been located by immunogold electron microscopy to the filtration slit, a technique which interferes quite drastically with the preservation of the specimens and does not yield the necessary spatial resolution to precisely determine the location of the respective proteins. We speculate that the protein composition of the two types of cell-cell contacts described in our present study only partially overlaps or may even be distinct from each other, so that there are different sets of proteins which belong to one type of cell-cell contact or another.

#### ACKNOWLEDGMENTS

We are very grateful for the careful segmentation of the data sets by Anita Hecht and Caroline Seebauer. Ton Maurer skillfully arranged the figures. The insightful comments of the reviewers were very helpful to better understand and interpret some of our results.

#### GRANTS

This work was supported by the German Research Council through SFB 699.

#### DISCLOSURES

No conflicts of interest, financial or otherwise, are declared by the authors.

#### AUTHOR CONTRIBUTIONS

Author contributions: T.B., F.H., M.P.K., and R.W. provided conception and design of research; T.B., F.H., C.M., and G.W. performed experiments; T.B., B.S., C.M., R.R., M.P.K., and R.W. analyzed data; T.B., C.M., H.-J.G., R.R., M.P.K., and R.W. interpreted results of experiments; T.B. and R.W. prepared figures; T.B., M.P.K., and R.W. edited and revised manuscript; T.B.,

F.H., B.S., C.M., H.-J.G., R.R., G.W., M.P.K., and R.W. approved final version of manuscript; R.W. drafted manuscript.

## REFERENCES

1. Dworak HA, Charles MA, Pellerano LB, Sink H. Characterization of *Drosophila hibris*, a gene related to human nephrin. *Development* 128: 4265–4276, 2001.
2. Hackl MJ, Burford JL, Villanueva K, Lam L, Suszták K, Schermer B, Benzing T, Peti-Peterdi J. Tracking the fate of glomerular epithelial cells in vivo using serial multiphoton imaging in new mouse models with fluorescent lineage tags. *Nat Med* 19: 1661–1666, 2013.
3. Höhne M, Ising C, Hagmann H, Völker LA, Brähler S, Schermer B, Brinkkoetter PT, Benzing T. Light microscopic visualization of podocyte ultrastructure demonstrates oscillating glomerular contractions. *Am J Pathol* 182: 332–338, 2013.
4. Ichimura K, Miyazaki N, Sadayama S, Murata K, Koike M, Nakamura Ki Ohta K, Sakai T. Three-dimensional architecture of podocytes revealed by block-face scanning electron microscopy. *Sci Rep* 5: 8993, 2015.
5. Kramer-Zucker AG, Wiessner S, Jensen AM, Drummond IA. Organization of the pronephric filtration apparatus in zebrafish requires nephrin, podocin and FERM domain protein Mosaic eyes. *Dev Biol* 285: 316–329, 2005.
6. Kremer JR, Mastrorarde DN, McIntosh JR. Computer visualization of three-dimensional image data using IMOD. *J Struct Biol* 116: 71–76, 1996.
7. Kriz W, Shirato I, Nagata M, LeHir M, Lemley KV. The podocyte's response to stress: the enigma of foot process effacement. *Am J Physiol Renal Physiol* 304: F333–F347, 2013.
8. Neal CR, Crook H, Bell E, Harper SJ, Bates DO. Three-dimensional reconstruction of glomeruli by electron microscopy reveals a distinct restrictive urinary subpodocyte space. *J Am Soc Nephrol* 16: 1223–1235, 2005.
9. Neal CR, Muston PR, Njegovan D, Verrill R, Harper SJ, Deen WM, Bates DO. Glomerular filtration into the subpodocyte space is highly restricted under physiological perfusion conditions. *Am J Physiol Renal Physiol* 293: F1787–F1798, 2007.
10. Reeves W, Caulfield JP, Farquhar MG. Differentiation of epithelial foot processes and filtration slits. Sequential appearance of occluding junctions, epithelial polyanion, and slit membranes in developing glomeruli. *Lab Invest* 39: 90–100, 1978.
11. Rodewald R, Karnovsky MJ. Porous substructure of the glomerular slit diaphragm in the rat and mouse. *J Cell Biol* 60: 423–433, 1974.
12. Ruotsalainen V, Patrakka J, Tissari P, Reponen P, Hess M, Kestilä M, Holmberg C, Salonen R, Heikinheimo M, Wartiovaara J, Tryggvason K, Jalanko H. Role of nephrin in cell junction formation in human nephrogenesis. *Am J Pathol* 157: 1905–1916, 2000.
13. Salmon AHJ, Toma I, Sipos A, Muston PR, Harper SJ, Bates DO, Neal CR, Peti-Peterdi J. Evidence for restriction of fluid and solute movement across the glomerular capillary wall by the subpodocyte space. *Am J Physiol Renal Physiol* 293: F1777–F1786, 2007.
14. Schneider CA, Rasband WS, Eliceiri KW. NIH Image to ImageJ: 25 years of image analysis. *Nat Methods* 9: 671–675, 2012.
15. Shankland SJ. The podocyte's response to injury: Role in proteinuria and glomerulosclerosis. *Kidney Int* 69: 2131–2147, 2006.
16. Tanaka T, Mitsushima A, Kashima Y, Nakadera T, Osatake H. Application of an ultrahigh-resolution scanning electron microscope (UHS-T1) to biological specimens. *J Electron Microscop Tech* 12: 146–154, 1989.
17. Tryggvason K, Patrakka J, Wartiovaara J. Hereditary proteinuria syndromes and mechanisms of proteinuria. *N Engl J Med* 354: 1387–1401, 2006.
18. Wartiovaara J, Öfverstedt LG, Khoshnoodi J, Zhang J, Mäkelä E, Sandin S, Ruotsalainen V, Cheng RH, Jalanko H, Skoglund U, Tryggvason K. Nephrin strands contribute to a porous slit diaphragm scaffold as revealed by electron tomography. *J Clin Invest* 114: 1475–1483, 2004.